HPGR Model verification and scale-up

M. J. Daniel*, S Morrell
Julius Kruttschnitt Mineral Research Centre, The University of Queensland,
Isles Road, Indooroopilly, Qld. 4068, Australia.

ABSTRACT

This paper summarises test results that were used to validate a model and scale-up procedure of the high pressure grinding roll (HPGR) which was developed at the JKMRC by Morrell, Tondo and Shi in 1996. Verification of the model is based on results from four data sets that describe the performance of three industrial scale units fitted with both studded and smooth roll surfaces. The industrial units are currently in operation within the diamond mining industry and are represented by De Beers, BHP Billiton and Rio Tinto. Ore samples from the De Beers and BHP Billiton operations were sent to the JKMRC for ore characterisation and HPGR laboratory-scale tests. Rio Tinto contributed an historical data set of tests completed during a previous research project.

The results conclude that the modelling of the HPGR process has matured to a point where the model may be used to evaluate new and to optimise existing comminution circuits. The model prediction of product size distribution is good and has been found to be strongly dependent of the characteristics of the material being tested. The prediction of throughput and corresponding power draw (based on throughput) is sensitive to inconsistent gap / diameter ratios observed between laboratory-scale tests and full-scale operations.

Keywords: comminution; high pressure grinding rolls; energy efficiency; model verification, scale-up.

- *Corresponding author. Tel. : +61-7-3365 5888; fax: +61-7-3365 5999
- *E-mail address*: m.daniel@uq.edu.au

1 Introduction

The turn of the millennium has awakened the developed world's interest in global energy consumption in view of the earth's limited fossil energy resources. So too have mining multinationals realised the serious impact that possible future energy limitations might have on the industry. The continued depletion of non-renewable energy resources has prompted a drive towards sustainability. To achieve this all sectors of the industrialised world will have to dramatically reduce energy consumption and increase energy efficiency. To this end, the mining industry has now taken up the challenge and is beginning to seek ways of developing sustainable mining practices. One particular area of focus is aimed at quantifying and modelling energy utilisation in comminution processes.

The High Pressure Grinding Rolls (HPGR) is a relatively new comminution device that offers realistic potential in dramatically reducing comminution energy requirements. As such, it is viewed as an alternative to the existing, less energy efficient processes such as semi-autogenous (SAG) and ball mills. (Morrell et al 1997) believed that an important factor in encouraging the use of the HPGR technology in the future, was through the availability of adequate process models for simulation that described the processes and scale-up requirements. Today simulation is widely used in mine pre-feasibility, feasibility and final design studies. However, the models behind comminution simulators such as JKSimMet, often rely on ore characterisation data and pilot scale test data for model calibration purposes. In HPGR evaluation, pilot scale tests require several tons of sample due to the high capacity of such units (50 – 80 t/h). By contrast laboratory-scale HPGR test units have much lower throughput capacities (1-5 t/h) which, if their results are scalable, are more cost effective, less labor intensive and enable the model to be calibrated using small amounts of sample. This is particularly suited to pre-feasibility studies where limited amounts of drill core are usually available. The issue of whether the results from a laboratory HPGR unit are scalable is particularly important. Hence a program was initiated to compare laboratory and full scale results using the Morrell, Tondo, Shi model.

Three different kimberlite ores were tested using laboratory-scale units fitted with both smooth and studded rolls. The laboratory-scale data was used to fit model parameters. The model was then used to scale-up to predict the performance of full-scale units treating the same ores. These simulated (predicted) results were then compared with the actual full-scale data as generated by each of the industrial scale operating units. Details of the operating ranges of the full scale machines are summarised in Table 1.

Table 1 Summary of the data sets used to validate the Morrell/Tondo/Shi HPGR model.

Data Source	Roll Surface	Roll Size (m)	kWh/t (full-scale)	kWh/t (lab-scale)
Rio Tinto (historical)	Smooth	2.2	1.8-2.5	1.8-2.5
De Beers	Smooth	2.8	4.0-4.5	4.0-4.5
De Beers	Studded	2.8	2.5-3.0	3.5-3.9
BHP Billiton	Studded	1.7	1.0-1.2	2.0-3.0

2 Overview of the HPGR

The basic machine concept is very simple. The material is force-fed into the unit by creating a head of material over the machine, as seen in Figure 1 (Napier-Munn, et al., 1996). Two counter-rotating rolls allow the compression breakage to be used in a continuous rather than batch operation.

One of the rollers in the HPGR rotates on a fixed axis while the other is allowed to move linearly with a pressing force applied to the moving roll. The moveable roller is forced up against the material in the gap between the rollers by an hydraulic oil cylinder system. This oil pressure acts through four or two cylinders (depending on the manufacturer) and transmits the grinding force over the cross-section of the diameter of the rolls where the bed has formed. The amount of material in the gap, or compression zone (> 50 MPa), may be manipulated to a limited degree to result in optimum operating conditions, but generally, it is a characteristic of the process ore, roll diameter and surface characteristics.

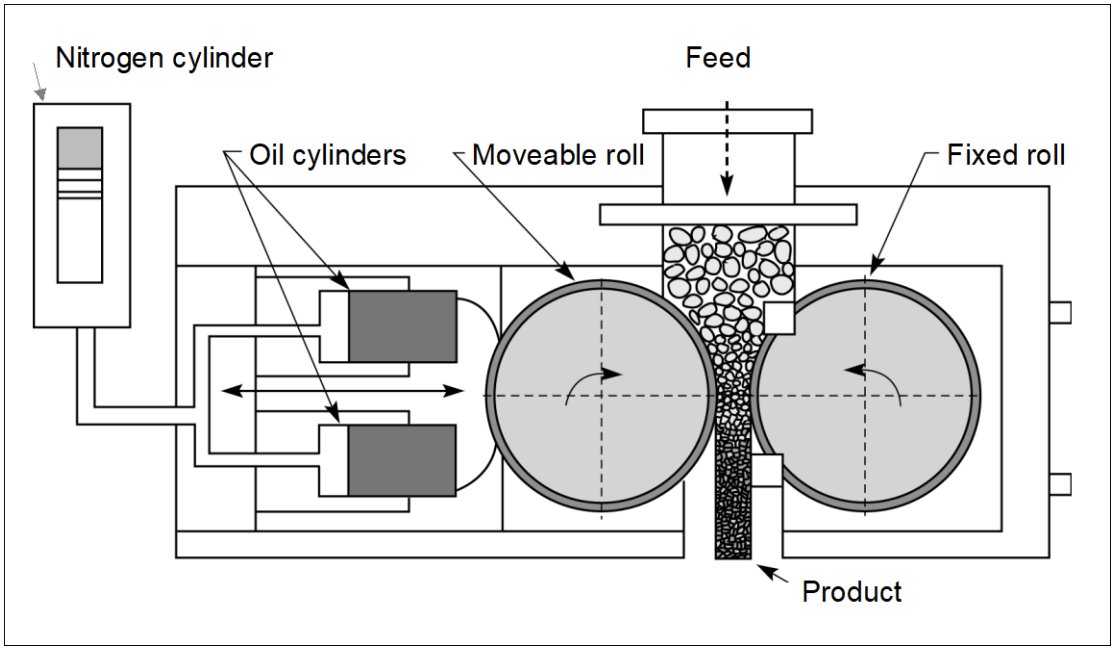

Figure 1 Cross sectional representation of HPGR, including the hydraulic spring system (Napier-Munn et al., 1996)

During processing, the particle bed is compressed to a density of greater than 70% solids by volume. The material is usually agglomerated into a cake (flake) that may have to be de-agglomerated before passing on to subsequent processes. This is achieved by either immersing the product in water in a sump under the discharge end of the rolls or by using a hammer, impact or ball mill (Schönert, 1988).

Ore is fed to the HPGR by means of a chute usually mounted directly above the gap between the rolls. Material is usually fine enough to be gravity fed into the HPGR (Schönert, 1988), where the nip angles of the particle and the internal friction of the bulk of the material mass are sufficient to continuously draw-in the material through the rolls.

The HPGR breaks particles predominantly in an autogenous way, unlike other comminution devices such as ball and rod mills. The grinding force is transferred from one particle to the next, with only a small proportion of the particles coming into direct contact with the rolls.

Schönert (1988, 1991) also mentions that even though the inter-particle process in less efficient than single particle stressing, he found that when a bed of particles is compressed and comminuted, the result is that the material is comminuted more efficiently than in a ball mill. Schönert concluded that the main reason for this is the fact that the controlled transport and stressing featured in HPGR results in a high proportion of available energy being used solely for the purpose of stressing the material. In conventional mills, the material transport and stressing inside the active volumes of the mill between the balls occurs randomly. This often allows particles to move out of position resulting in unproductive collisions between grinding media and the liner wall within the mill. This mode of energy input is inherently wasteful because of the hit-and-miss nature of the process.

3 Model structure and theory.

The Morrell/Tondo/Shi model consists of three parts, namely a model for the prediction of product size distribution, a throughput model, and a power consumption component. The throughput model component uses a standard plug flow model version that has been used extensively by the manufacturers and researchers. The power consumption is based on the throughput and the specific comminution energy (E_{cs}) input.

3.1. Modelling Particle Size Distribution

Modelling the product size distribution also comprises three separately defined processes that are each modelled and then combined to produce a final result. The size reduction model relies on the assumption that the three breakage mechanisms occur independently within the HPGR (Morrell et al, 1997). These sub processes or zones within the crusher are defined as

(i) the pre-crusher zone,
(ii) the edge effect zone and
(iii) the compression zone.

The zones are described conceptually in Figure 2.

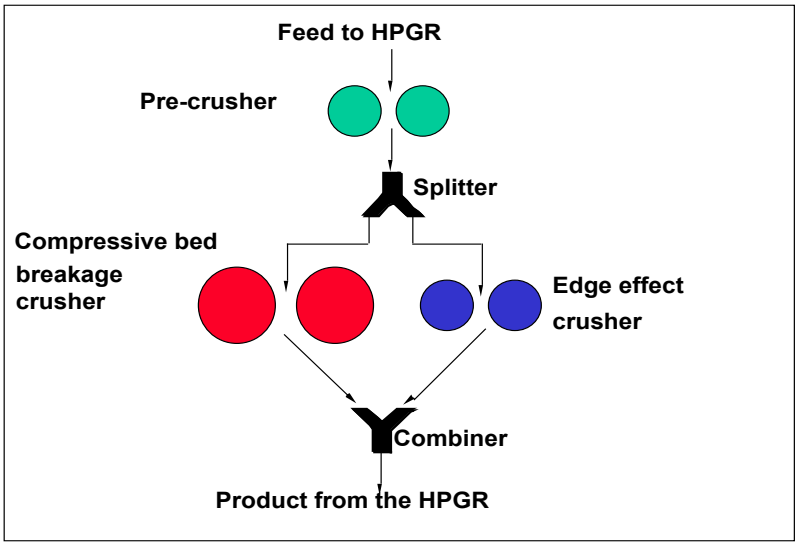

Figure 2 The current Morrell/Tondo model structure represented conceptually (Morrell et al., 1997).

3.1.1. The "pre-crusher" zone

If particles are bigger than a certain critical size (x_c), they will be broken directly by the roll faces as would occur in a conventional rolls crusher. The product of this pre-comminution process then passes into a region where a bed under compression has formed. Thus the interface between the compression and pre-crusher zones is defined by the critical gap (x_c), and is expressed as:

$$x_c = 0.5\left\{\left(D + x_g\right) - \left[\left(D + x_g\right)^2 - \frac{4\rho_g D x_g}{\rho_c}\right]^{0.5}\right\} \quad (1)$$

where, D = roll diameter (m),
x_g = working gap (m),
ρ_g = flake density (t/m^3),
ρ_c = bulk "compacted" density (t/m^3)

3.1.2. The "edge effect" zone

Breakage at the edge of the rolls is different to that at the centre and conforms more to that experienced in a conventional rolls crusher. This so-called "edge effect" is what defines the proportion of relatively coarse particles usually seen in HPGR products. Its existence has been explained by the pressure gradient across the width of the roll and the zero confinement of the ore at the edges of the rolls where cheek-plates are sometimes provided (Watson and Brooks, 1994).

The model assumes a step-change in pressure profile at the rolls edge where material is comminuted in single particle mode similar to the pre-crusher zone. No compressed bed breakage is assumed to take place in this zone, whereas in reality a gradual change in pressure is likely to be encountered.

The interface which defines the boundary between the compression zone and the edge effect zone is represented mathematically by a fraction of the original feed material which undergoes the single particle comminution. This fraction is represented by equation 2 (Morrell et al, 1997).

$$f = \gamma \frac{x_g}{L} \tag{2}$$

where, f = the fraction of the feed material which is comminuted in the edge zone
γ = "ore specific" split factor
x_g = working gap (m),
L = length of the rolls (m)

3.1.3. The "compression" zone

The compression zone boundary is at some point away from the outer edges of the rolls, defined by *f/2.L*, where L is the length of the rolls and f the fraction defined by equation 2, and extending upwards from the area of minimum gap (x_g) to the area bounded by the critical gap (x_c) given by equation 1. The compression zone is by far the most important comminution zone, as it is in this region where the majority of the breakage processes take place.

3.2. Throughput

The measured (experimental) throughput is determined by dividing the sample test mass by the time to process (equation 3) and is expressed in tonnes per hour (t/hr).

$$Q_m = 3.6 \frac{Test\ Sample\ mass(kg)}{Time\ to\ process(\text{sec})} \tag{3}$$

The model predicts throughput using equation 4 and is also expressed in tonnes per hour (t/hr).

$$Q_c = 3600 U L \rho_g x_g c \tag{4}$$

where, U = circumferential rolls speed (m/s),
L = rolls width (m),
x_g = working gap (m)
ρ_g = density of the flake produced (t/m^3)
c = correction factor

3.3. Power draw

The power draw (kW) for a simulated HPGR is calculated directly from the product of the specific comminution energy (E_{cs}) measured during the laboratory (kWh/t) and the predicted throughput (*t/h*) of the simulated HPGR. The power draw prediction is therefore directly related to the accuracy of the throughput prediction.

The experimentally measured specific energy (E_{cs}) is calculated from the sum of the measured shaft power (P_{shaft}) and the no-load power, divided by the measured throughput (Q_m) as expressed in equation 5.

$$E_{cs} = \frac{(P_{no-load} + P_{shaft})}{Q_m} \quad (5)$$

The shaft power (P_{shaft}) is calculated from the experimentally measured torque (τ) on the rolls along with the circumferential speed of the rolls expressed in equation 6. The no-load power ($P_{no-load}$) is the power consumed by the unit when no material is being fed.

$$P_{shaft} = \frac{2\tau u}{D} \quad (6)$$

where, τ = shaft torque (N.m)
u = circumferential speed (m/s)
D = rolls diameter (m)
P_{shaft} = net shaft power (kWh/t)

4 Experimental Program

4.1. Background to experimental test work

The test work consisted of a series of experiments conducted with a range of ores using a laboratory-scale HPGR. The results of these tests and the associated experimental errors were used to first calibrate the HPGR model. The same model parameters determined from the calibration process are used during scale-up to simulate the performance of a full-scale unit.

The overall result was that three new data sets were generated using the two different kimberlite ores. The fourth data set was a historical data set that was acquired during a previous project. Here data with similar specific energies to the full-scale and pilot scale operation were extracted from the data set to produce the Rio Tinto modelling data set.

The De Beers industrial unit was first operated with smooth rolls. These were replaced with studded rolls during the course of the project. As a result an additional data set was generated, and a direct comparison between the performance of smooth and studded rolls surfaces was made. Studded rolls, are seen as a standard feature in new designs (Figure 3), because of their improved wear resistant characteristics (Battersby 1992).

Figure 3 Typical full-scale roll surface characteristics, welded, chevron, studded and hexadur.

Studded rolls also improve process performances through higher throughput rates and an apparent lower specific energy consumptions (Lim and Weller 1997 b). The full-scale BHP Billiton unit is a unit fitted with studded rolls, and so in order to make a direct comparison between the two types of roll surface designs, it was necessary for the research project to complete tests on a laboratory scale unit fitted with both smooth and studded rolls.

4.2. Relative scale of the test unit to full-scale units

The industrial-scale data sets represent the performance of units with roll diameters of 1.7 m, 2.2 m and 2.8 m. Figure 4 shows the relative scale of the three industrial units, the JKMRC conventional 300 mm rolls and the Amdel 250 mm HPGR rolls. Two geometrically similar particles are placed between a full-scale roll and a laboratory-scale test unit to amplify the relative positions where particles first make contact with the rolls surface. This affects both nipping of individual particles in the pre-crusher zone. The relative voidage between particles in the laboratory-scale feed is assumed to be similar to the full-scale feed voidage conditions. This implies that the bulk density is the same for both laboratory scale and full-scale.

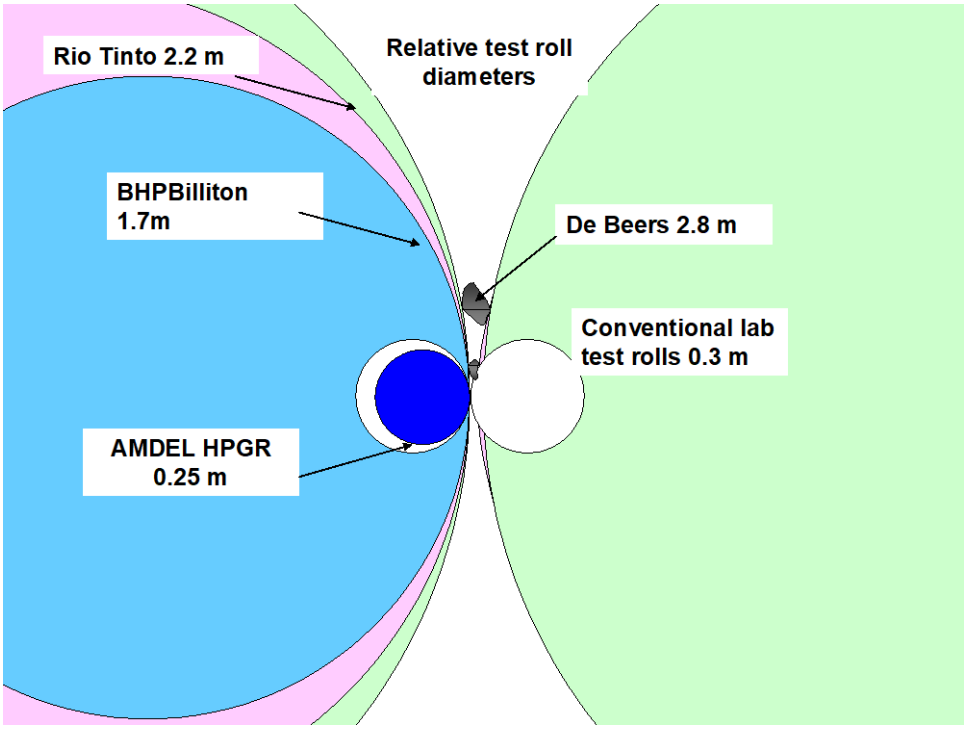

Figure 4 shows the relative gap and rolls diameter between industrial scale units and the laboratory-scale unit.

4.3. The Amdel laboratory-scale test unit

The Amdel laboratory-scale unit (Figure 5) employed for the test work was a unit originally manufactured by Krupp Polysius and shows both the smooth and studded roll profiles. The rolls are 100 mm wide and have a diameter of 250 mm. Each roll is independently driven by a separate motor which has the option of two fixed speed settings of 0.33 m/s and 0.67 m/s. Also depicted in Figure 4.3.1 is the feed chute/hopper which is used to maintain a constant head of feed material to the HPGR.

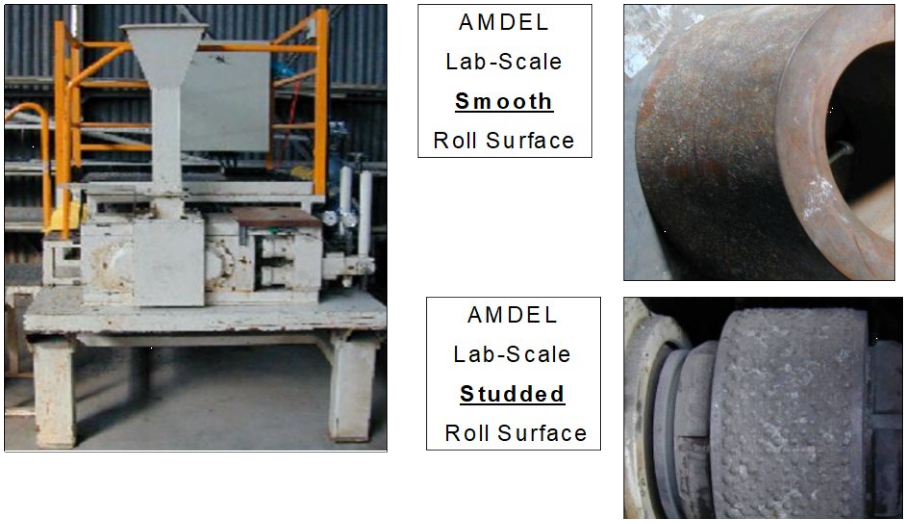

Figure 5 The 250 mm Amdel test unit fitted with both smooth and studded rolls surface profiles.

4.4. Test data (measurements) required by the model.

Verification of each of three model components formed a structured basis for the data/ measurements that were required during the experimental phase.

- Scale up procedure (scaling data, ratio of roll diameter and working gap)
- Prediction of throughput.
- Prediction of power draw
- Prediction of product size distribution, including :

    - (i) Fraction of material split to compressed bed zone and edge effect,
    - (ii) Single particle breakage – appearance function
    - (iii) Compressed bed breakage – appearance function
    - (iv) Default model parameters

The data required by each of the above model components may be further categorised into five groups. The groups are shown in Table 2 and Table 3 and constitute all the data needed for the model verification procedure.

Table 2 Model data derived from experimental measurements.

Item	Data category	Model data (Experimental measurements)
1	Measured input	Sample mass Roll diameter (D), Roll width (L), Roll speed (U) Bulk "compacted" density (ρ_c), Feed size distribution,
2	Measured output	Working gap (x_g), Flake thickness (x_{gf}),(Flake density (ρ_g) Product size distribution (measured), Batch process time Working pressure (p_w), Power (kW)

Table 3 Model parameters and calculated outputs

Item	Data category	Model parameters and calculated output
3	Calculated output	Measured throughput (Q_m), Calculated throughput (Q_{calc}) Specific Energy (E_{cs}), Specific Force (F_{sp}) Critical gap (x_c), Product size distribution (calculated)
4	Fixed default parameters	t_{10p}, $t_{10e,}$ $K1_p$, $K2_p$, $K3_p$, $K1_e$, $K2_e$, $K3_e$, $K1_h$, $K2_h$, $K3_h$ Split factor (γ), $K_{p\ (Edge)}$)
5	Critical model parameters	Power coefficient ($K_{p\ (HPGR)}$), t_{10h}

4.5. Calibrating the model & scaling-up.

To verify the model's scale-up ability, the procedure followed was first to calibrate the model using data from tests completed on a laboratory-scale unit. Calibration was achieved by fitting a curve to the experimental product size distribution. The calibrated model parameters were then fixed and a particular specific energy input used. To predict the outputs of a full-scale unit with the same specific energy, the predicted outputs were compared to the actual full-scale performance data. This procedure is summarised in Figure 6.

Calibrating the model requires only a single data set from a single test. The model may then only predict the full-scale performance using a similar specific comminution energy.

Ideally, a test series of at least five to six tests which have a range of specific energies and corresponding product size distributions are needed. Each of these data sets generated from the test series may be model-fitted to determine how the two critical model parameters t_{10h} and $K_{p(hpgr)}$.(power coefficient) interact. An example of this interaction is shown in Figure 5.2, where the parameter $K_{p(hpgr)}$ is shown to increases with increasing energy input, whilst keeping t_{10} constant. When the t_{10} parameter is kept constant, the resultant predicted product size distribution approximates (ie with large residual errors) the measured product size distribution. When t_{10} is not fixed and is fitted with K_{phpgr} , then it was found that similar fitted t_{10} values were obtained. Generally, the t_{10} parameter is found to remain numerically in the range of 30 to 40 for all ores tested. This phenomenon was observed and reported previously by Morrell et al (1997), Lim and Weller (1997), Fuerstenau et al (1991, 1993) and Schönert (1988) as a "self-similarity effect", where increased energy input resulted in the parallel shift towards a finer product size distribution. The power coefficient reflects the utilisation of applied power in size reduction (a higher value of $K_{p(hpgr)}$ reflects poorer energy utilization).

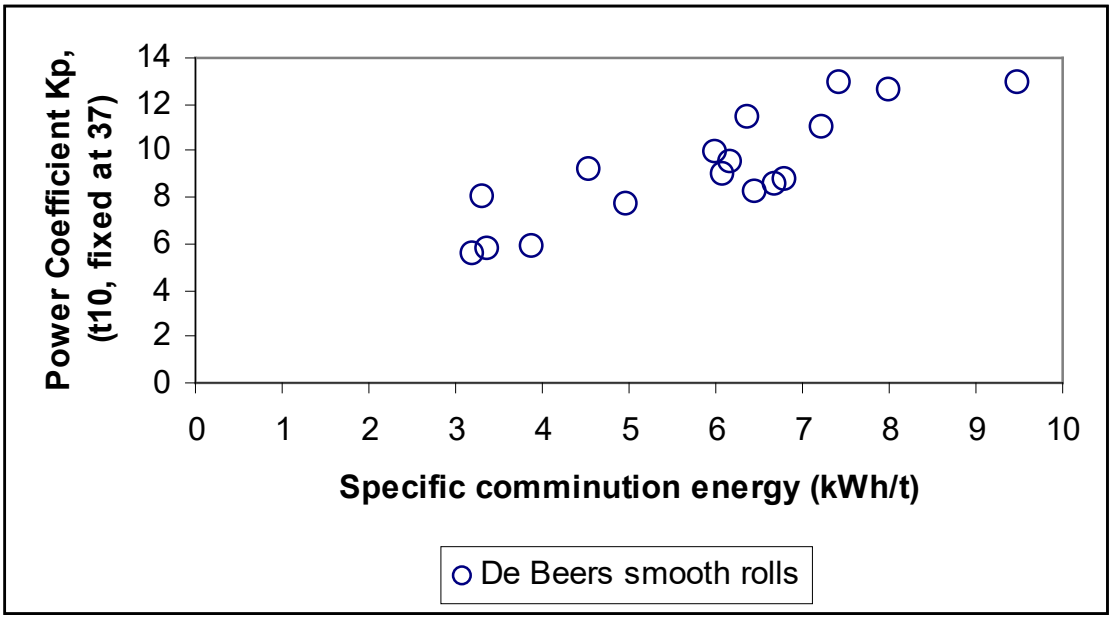

Figure 6 shows the specific comminution energy (kWh/r) vs. power coefficient ($K_{p(hpgr)}$), (where t_{10} is kept constant)

By fixing the t_{10} parameter, it was possible to establish that a linear relationship between the power coefficient $K_{p(hpgr)}$ and specific energy (kWh/t) exists. The model fitted product size distribution had a larger error in these cases than the error obtained when allowing the t_{10} parameter to be fitted as a second model parameter. The data was however produced to provide the general linear relationship that exists between $K_{p(hpgr)}$ and E_{cs} as shown in Figure 6, which enabled the model to linearly adjust the $K_{p(hpgr)}$ value during scale up. This adjustment of the $K_{p(hpgr)}$ value is necessary when the laboratory-scale specific energy differs from the full-scale specific energy. The adjustment makes allowances for the portion of energy that is converted into heat energy after the energy

saturation point has been reached. The point at which maximum size reduction occurs is described as the saturation energy (Tondo, 1997).

Once the model has been calibrated, all model parameters are subsequently fixed and used in the full-scale simulation. The "new" diameter of the simulated mill (full-scale) is used with other variables such as rolls speed, and flake and bulk density, and is "scaled up" when the simulation is run.

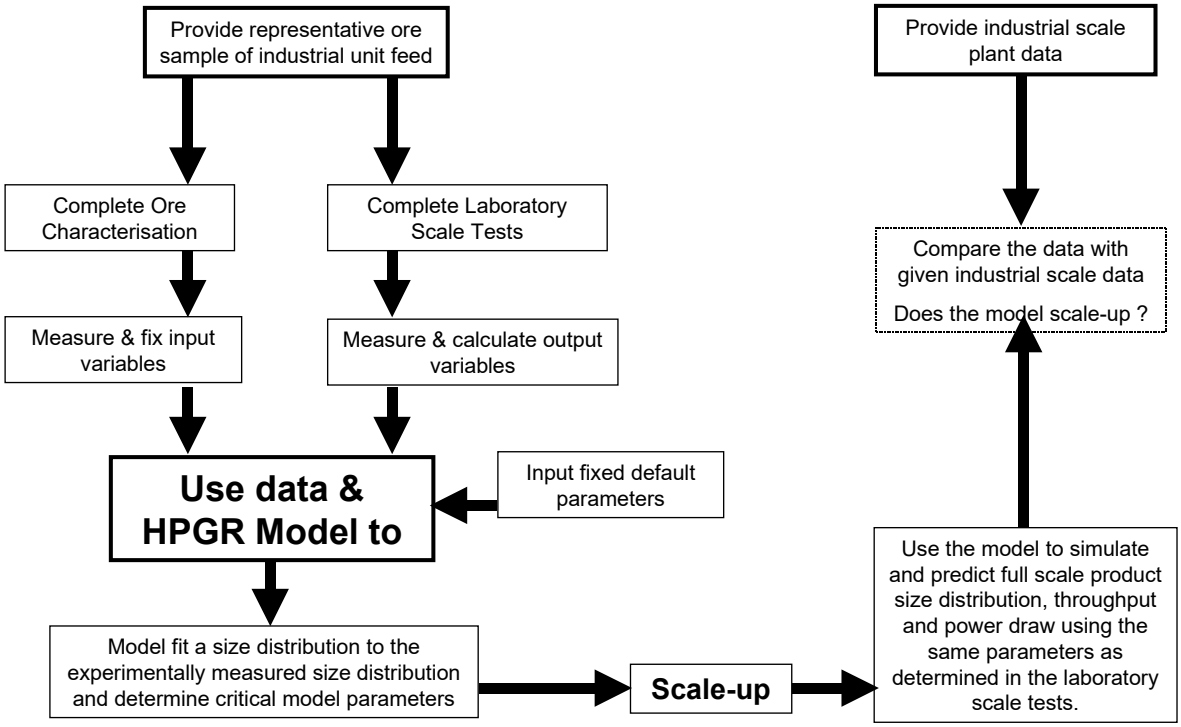

Figure 7 shows the procedure for the HPGR model verification and scale-up.

During scale-up, the model uses a scale factor to predict the working gap of the simulated mill. The working gap of the original laboratory-scale mill is multiplied by a scale factor to calculate the working gap of the simulated full-scale mill. The scale factor is defined as the ratio of the simulated mill diameter divided by the original mill diameter and expressed in equation 7.

$$Scale\ factor = \frac{D_{simulated}}{D_{original}} = \frac{D_{full-scale}}{D_{lab-scale}} \qquad (7)$$

Hence it is the laboratory-scale working gap, that when multiplied by the scale factor determines the full-scale working gap. The scale-up procedure relies on the assumption that gap / diameter ratio is constant during scale-up. This assumption is known in literature to be poorly understood, but remains true within a limited range. For example diameter to gap ratios have been reported to remain between 0.9% and 1.6%, which relative to the rolls diameter is not seen as significant, but dramatically changes

throughput estimations when the working gap is amplified by the scale factor in full-scale units. When the scale factor is large (e.g. 11.2), the accuracy of gap measurement at lab scale becomes critical to the performance of the throughput model and the resultant power draw.

5 Results

5.1. Working gap

The measured versus predicted full-scale working gaps (calculated from the working gap of the experimental test) are shown in Figure 8. The De Beers smooth roll working gap was reported to be 24 mm, although no actual measurement of the gap was believed to have been made. The design working gap for this unit is 31.5 mm which is comparable to the predicted working gap, as determined by scale up from the experimental working gaps.

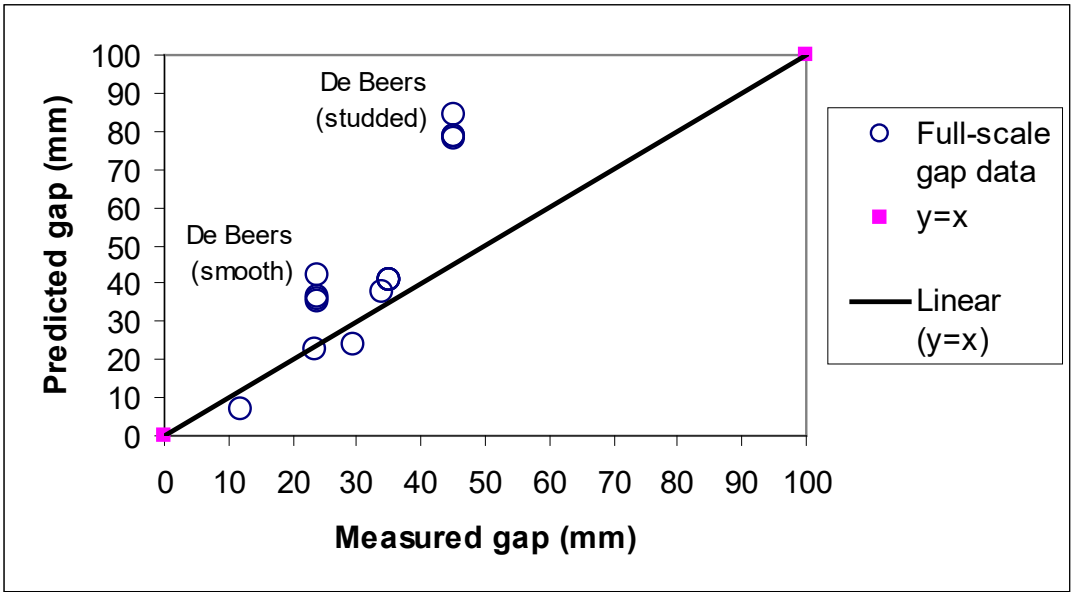

Figure 8 Measured versus predicted full-scale working gaps.

The De Beers studded working gaps (Figure 8) were measured accurately during the commissioning tests of the new studded rolls (gap measurement represent stud to stud). Here, the predicted studded working gap is believed to be in error due to the difficulty in measuring a "studded" working gap during the laboratory tests.

A further limitation of the model scale-up is realised when the parameters t_{10} and K_p as determined during model calibration are used in full-scale simulation. As mentioned previously, the simulated prediction is only valid when an identical specific energy input to that which was measured during laboratory-scale tests is used. This point highlights the need to complete a series of laboratory-scale tests with a range of specific energy inputs.

The results may then give an indication of the saturation energy level, and the results from this test should then be chosen for scale-up.

5.2. Throughput.

The measured (experimental) throughput versus calculated (model) throughput of a series of laboratory-scale tests is shown in Figure 9. The graph displays the 99% and 95% confidence limits generated from a statistical linear comparison method.

The errors associated with the fittings are also shown in the figures. These errors reflect the accuracy of the fits and were calculated using equation 9.

$$Error = \sqrt{\frac{\sum_{i=1}^{N}\left(\frac{y_{mi} - y_{pi}}{y_{mi}}\right)^2}{N}} \qquad (8)$$

Where N = number of data sets

y_{mi} = the i^{th} measurement (individually fitted) value

y_{pi} = the i^{th} prediction (model) value

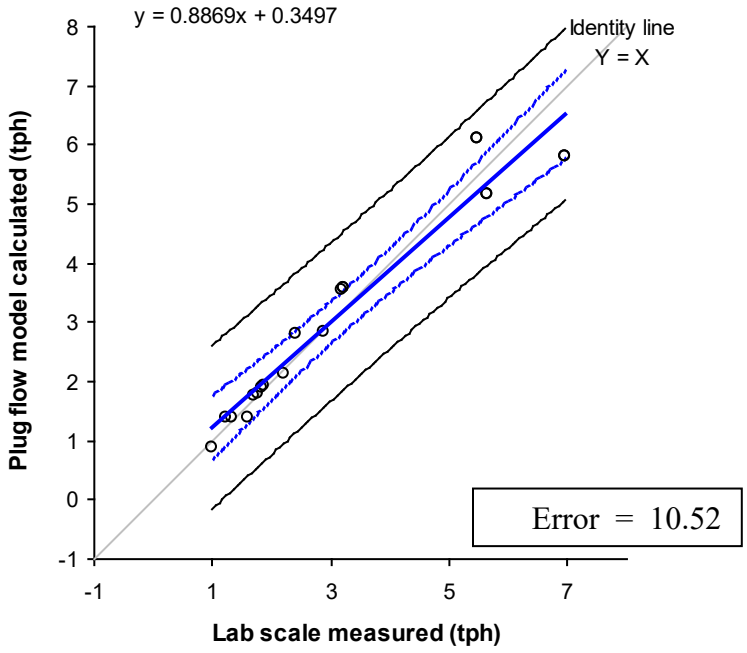

Figure 9 Measured throughput versus calculated model throughput for tests completed on the laboratory-scale unit.

Figure 9 shows that the throughput model works well when accurate measurements of the model variables have been made. In this case the measured flake thickness and corresponding flake density was used as described in equation 4. The velocity of the rolls was the same as the velocity of the bed exiting the rolls as no material slip is deemed to be taking place. This conclusion has also recently been published by Schönert (2001). Thus possible variations in throughput could be attributed to the error in experimental measurements of the flake, gap and rolls speed or in the error caused by the lower density of the material in the edge effect zone. The error in resultant measured and calculated throughputs ranged from –16.8% to 16.5%, and the overall error of the model based on the available experimental data was 10.52 %.

Equation 3 was then applied to the full-scale data (Figure 10) where two very noticeable outliers are present that represent the throughput of the Rio Tinto unit. In this particular case the measured throughput far exceeds the predicted throughput. This is thought to have been due to the state of the cheek plates. These plates are used to prevent material from by-passing the rolls and had worn away during the time of data acquisition.. This caused excessive feed material to spill out from the sides of the rolls resulting in the high throughputs as measured on the feed conveyor. The actual feed which was comminuted between the rolls would have been much less.

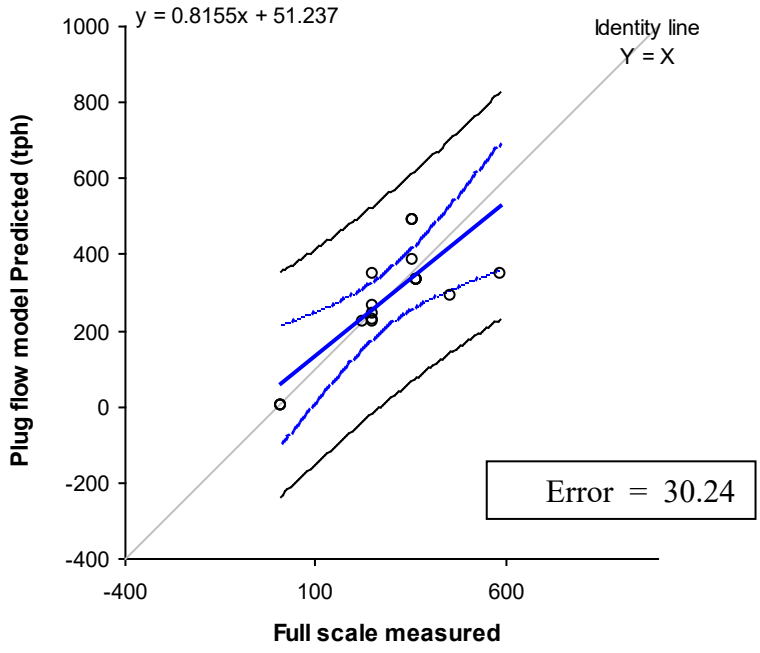

Figure10 Measured industrial scale throughput versus scale-up predicted throughput for three sets of data

Figure 10 shows the relationship between the measured and predicted throughputs. The graph displays the 99% and 95% confidence limits generated from a linear comparison method. The error in the measured experiments (excluding the outlier) is still high and ranged from –38 % to 39%. These high values are as a result of the

inconsistencies in the gap/diameter ratios that are observed during the scale-up from laboratory-scale to full-scale and the difficulty in being able to measure accurately the working gap.

Measured and calculated throughputs are usually compared to determine how accurate the model expression is. Variations between the measured and calculated throughput may be attributed to variations in the density of the material in the edge effect zone and the compression zone coupled with the expansion effect between materials in the gap to that which has exited the gap. Errors in the measurement of the rolls speed and gap width could also attribute to throughput discrepancies. These areas where experimental errors are possible are the root cause for discrepancies between measured and calculated throughputs.

Currently, the diameter / gap ratio is assumed to be constant during scale-up and is used to predict the full-scale working gap. Full-scale working gap is calculated by multiplying the laboratory-scale working gap by the ratio of the roll diameters (full-scale to laboratory-scale). This assumption, coupled with the error in the measurement of laboratory-scale unit working gap may result in large discrepancies between the actual and predicted working gap at full-scale. These differences may cause misleading calculated throughputs and associated power draw.

5.3. Power draw.

A unique feature of the Morrell/Tondo/Shi model is the way in which one of the Whiten model parameters ($K3_h$) for the compression zone is determined. Before model calibration and scale-up may continue, the model first requires an input value for the specific comminution energy. The value of the specific comminution energy is calculated by dividing the shaft power that was measured during the experiment by the throughput rate (time to process a known mass of material).

The specific comminution energy is usually fixed during scale up, unless it is required to predict the product size distribution at a different specific comminution energy. During model calibration (using the measured specific comminution energy) the model parameter $K3_h$ is determined iteratively so that the model predicts the calculated power required that matches the power required as determined by the required throughput and the specified specific comminution energy.

This method ensures that the plant power and model calculated power draw required by the motors of a HPGR unit are always the same. However since the model relies on a good estimate of the specific comminution energy which is determined through the measurement of the torque on the rolls and the measured throughput. So unless the throughput and torque measurements are indeed accurate, the resultant calculated power draw will not be correct. This is shown in the predicted laboratory-scale power requirements in Figure 11 and the corresponding discrepancies in full-scale power predictions shown in Figure 12 The graph displays the 99% and 95% confidence limits

generated from a linear comparison method. The model error for the laboratory scale power draft prediction was 14,0 % and 30.4 % for the full-scale power draft.

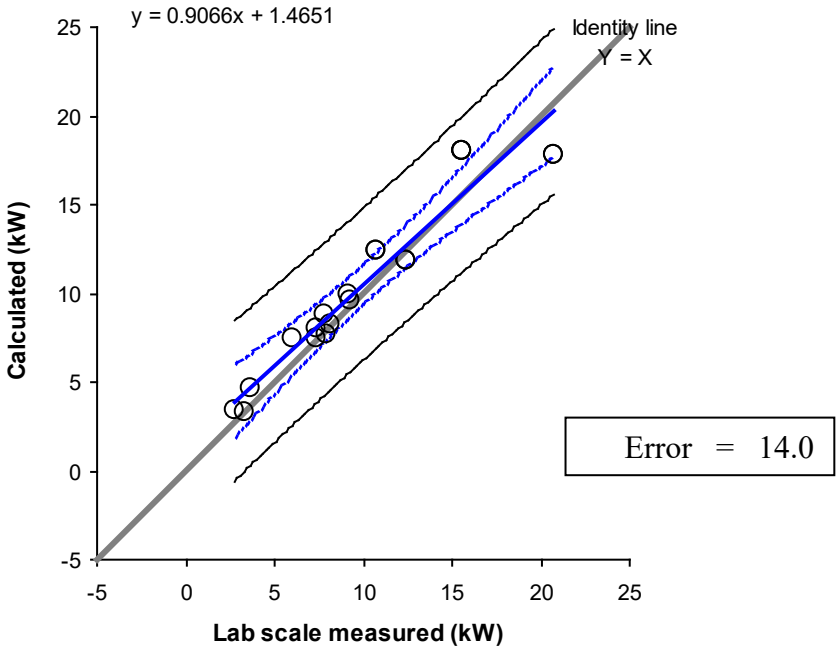

Figure 10 shows measured versus calculated power draw for experiments completed on the laboratory-scale test unit.

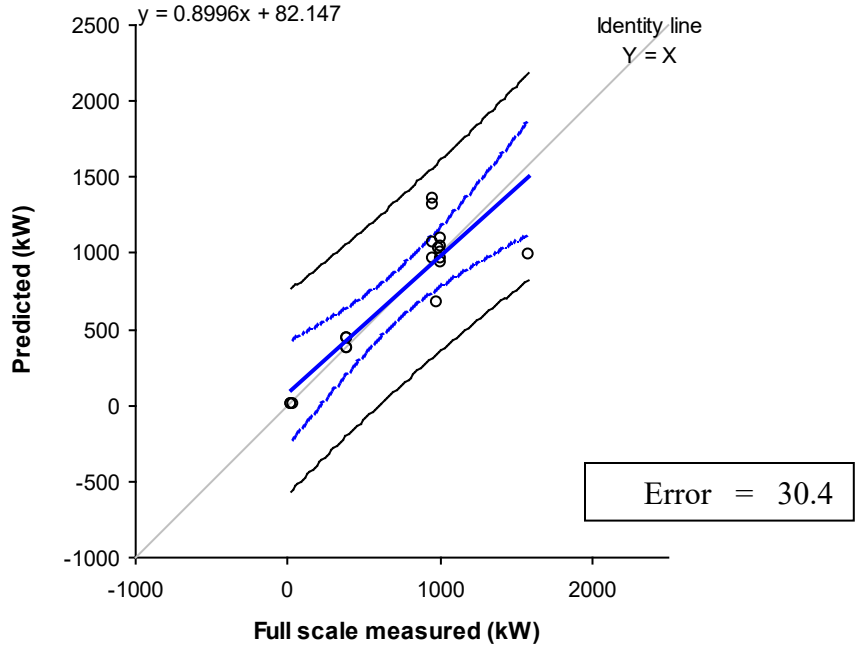

Figure 12 shows measured versus calculated power draw in full-scale predictions based from experimental results completed on a laboratory-scale unit.

Again the outlier representing the Rio Tinto unit, has a large discrepancy between the measured versus predicted power draw. This has been caused by the throughput discrepancy explained previously, and the fact that the actual specific comminution energy should be higher in the full-scale unit, than that which has been reported.

These results show hat the prediction of throughput and power draw is sensitive to experimental measurements such as the working gap (flake thickness). In studded or profiled rolls the measurement of the effective gap is difficult and is further complicated by having to estimate the average thickness of the flakes produced. Sometimes the effective gap is defined by measuring the gap as the distance between the rolls from stud to stud which may cause bias in calculated throughputs. In addition to this, knowledge of full-scale and laboratory-scale process anomalies such as feed material by-pass or working gap estimations needs to be taken into account when using the model.

5.4. Calculated (predicted) product size distribution and scale-up

The model fitted and experimentally measured product size distribution results for each of the units/ores tested are shown as the left hand side graphs of Figures 13(a)-16(b). The simulated prediction of the full-scale unit performance versus the actual industrial scale data for the four units being used to verify the model are shown in the right hand side graphs of Figures 13(b) to 16(b). What is noticeable in producing these results is that the feed size distributions that were prepared were geometrically similar to the full scale feed size distribution. These tests produced similar predicted product size distributions, but the results were not as accurate as those tests where the replicated "geometrically similar " feed size distributions were used.

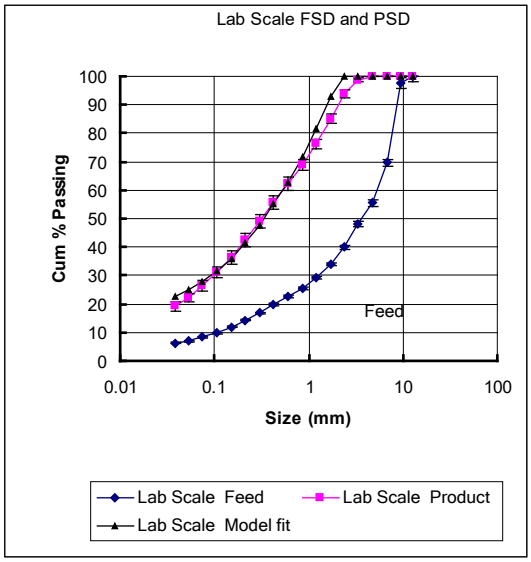

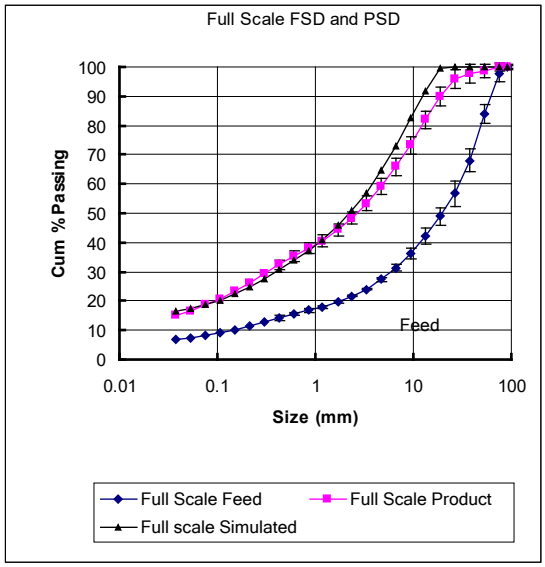

Figure 13(a) Model fitting to experimental PSD for Rio Tinto 0.25 m smooth rolls at 2.2 kWh/t.

Figure 13(b) Scale-up and model verification using the Rio Tinto 2.2 m smooth rolls at 2.28 kWh/t.

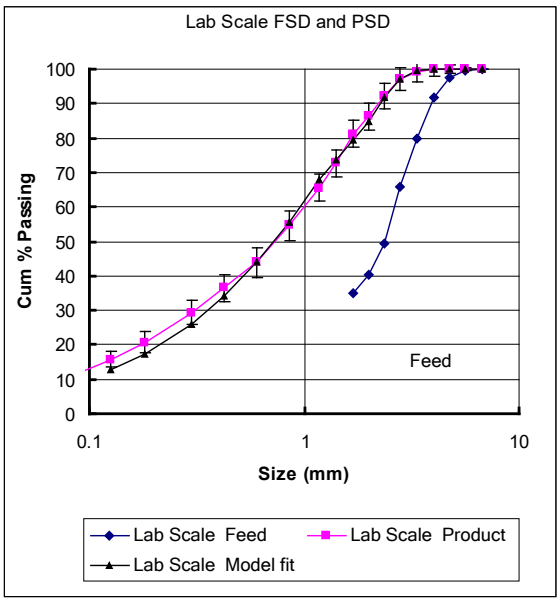

Figure 14(a)

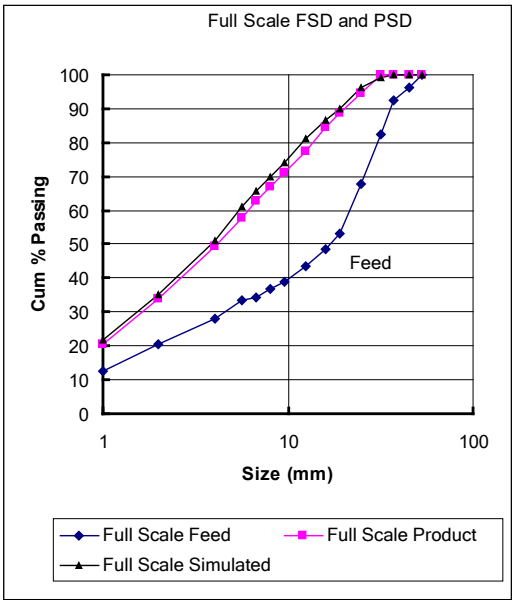

Figure 14(b)

*Figure 14(a) Model fitting to experimental PSD for De Beers, using 0.25 m **Smooth** rolls at 3.3 kWh/t.*

*Figure 14(b) Scale-up and model verification of the De Beers 2.8 m **Smooth rolls** at 4.0 kWh/t.*

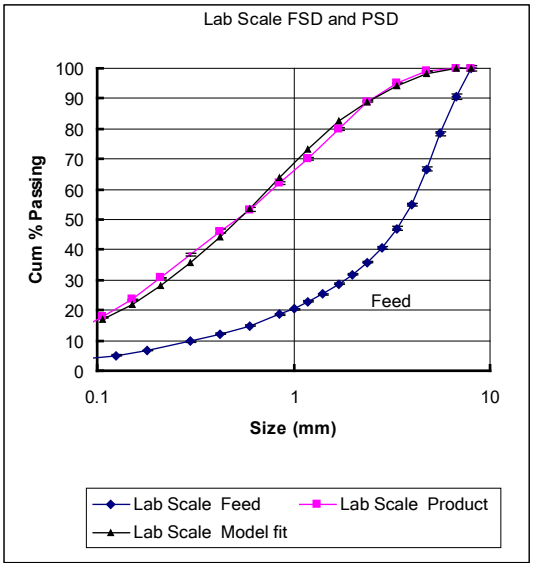

Figure 15(a)

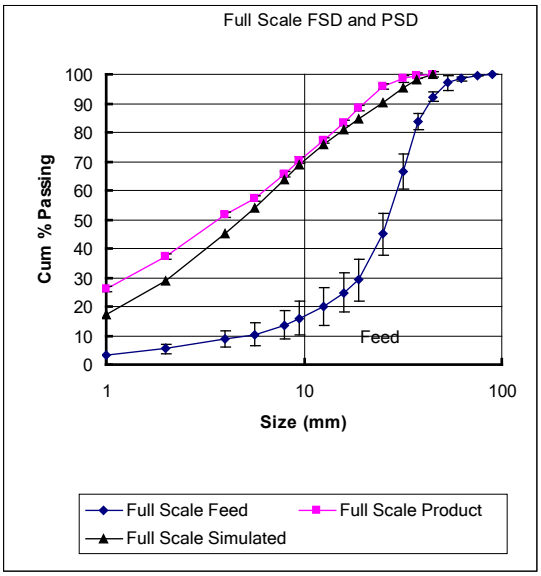

Figure 15(b)

*Figure 15(a) Model fitting to experimental PSD for De Beers, using 0.25 m **Studded** rolls at 4.9 kWh/t.*

*Figure 15(b) Scale-up and model verification of the De Beers 2.8 m **Studded** rolls at 2.67 kWh/t .*

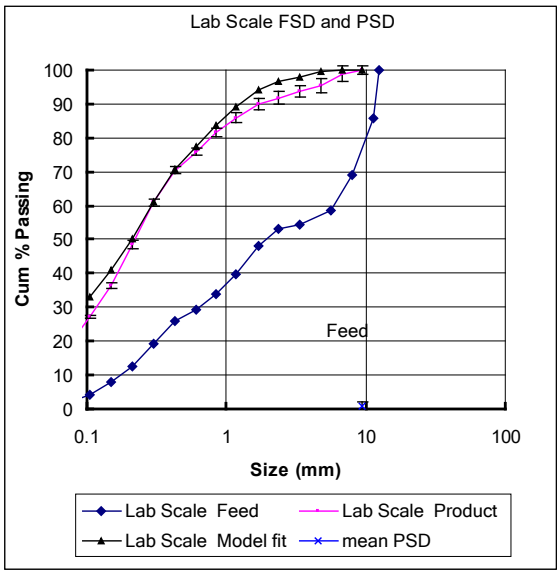

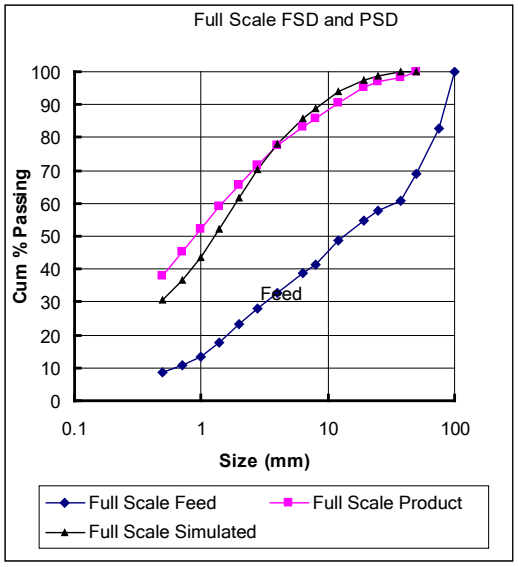

Figure 16(a) *Figure 16(b)*

Figure 16(a) Model fitting to experimental PSD for BHP Billiton, using 0.25 m Studded rolls at 2.03 kWh/t

Figure 16(b) Scale-up and model verification of the BHP Billiton 1.7 m Studded rolls at 1.08 kWh/t.

In the BHP Billiton series, the model is fitted to the product size distribution of a test which had a measured specific energy of 2.03 kWh/t. The model fitting calibrated the model and produced a similar product size distribution using a t_{10} of 53, and $K_{p(hpgr)}$ of 1.77. The full-scale data was representative of an energy input of 1.08 kWh/t. Since the energies were not the same it was therefore assumed that the energy saturation point (energy level where maximum size reduction takes place) had already been reached, and a linear adjustment to the $K_{p(hpgr)}$ parameter is justified. Simulation then used an identical t_{10} value of 53, but a new (linearly adjusted) $K_{p(HPGR)}$ parameter of 0.94 was used representing an energy input of 1.08 kWh/t.

Running the full-scale simulation resulted in a predicted product size distribution that is very similar to the flake size distribution of the full-scale industrial data. If this procedure is to be used, extreme care must be taken when using the adjusted parameters. In order to avoid having to do this it is recommended that a series of tests be completed to determine where the energy saturation point is. This not only provides more data with which to simulate a new mill, but provides the operator with valuable information as to how the process might be optimised. All operations using HPGR should aim to operate their units at or near the energy saturation level for maximum comminution benefit.

6 Conclusions

The results conclude that the modelling of the HPGR process has matured to a point where the model may be used in JKSimMet to evaluate new and to optimise existing comminution circuits. The model prediction of product size distribution is good and has been found to be strongly dependent of the characteristics of the material being tested and is said to be ore specific.

The prediction of throughput and corresponding power draw (based on throughput) is sensitive to inconsistent gap / diameter ratios observed between laboratory-scale tests and full-scale operations. The current throughput model appears to be accurate and reliable only when accurate measurements of the gap are made when treating geometrically similar feed size distributions operating at low circumferential speeds. The correction factor used to offset the effect of the so called material slippage at higher circumferential speeds was not evaluated as part of this study. However, consideration to the manufacturers roll speed scale-up rules appears to produce reliable scale-up performance predictions, and therefore no need seen to complete laboratory-scale tests at high circumferential speeds. Since the model's power draw is directly proportional to the throughput, the resultant accuracy of the power draw is therefore directly dependent on the accuracy of the throughput as described above.

A characteristic feature of HPGR process is that the comminution takes place only up to a certain limiting point, beyond which little or no further comminution is realised. The process was observed to continue consuming energy after the maximum comminution benefit had been reached. This energy is wasted by the process and is converted mainly into heat. This heat is likely to be caused by the very high frictional forces that begin to dominate the process when the majority of the internal voids between particles have collapsed and the material becomes incompressible.

Under normal HPGR process conditions the edge and pre-crusher model component are not dominant, but contribute to the accuracy of the overall model. Model parameters are a function of the ore, hence there is a need to complete laboratory-scale tests, in order to predict the performance of a full-scale unit with a particular ore.

The latest technological improvements in HPGR rolls surface design and materials by the manufacturers coupled with proven process models will now hopefully encourage the wider minerals industry to further adopt this technology. The model may now be used to justify the existence of the HPGR in various comminution circuit scenarios based on the accurate predictive performance of such units performance

7 Recommendations

It is recommended that the data requirements for HPGR modelling and scale up be obtained from only ore characterisation tests conducted within in a piston and die. The test procedure should be researched to include measurements that may be related to a power prediction model. In addition to this the working gap prediction should be based on ideal hydraulic system settings as determined by the tests.

It is recommended that the suggested minor modifications to the exciting throughput model be tested and statistically evaluated based on the knowledge that slip within the gap is not possible (Schönert and Sander 2000, 2001). This analysis should include the effect of the suspected flake expansion after it exits the compression zone.

Finally, mineral liberation should be researched and measured either as a function of the amount of fines generated, or as a function of the product size distribution relative to the valuable mineral size distribution component of the ore. These indicators could eventually become the overriding measures which may determine the performance conditions at which the HPGR should be operated.

ACKNOWLEDGEMENTS

Acknowledgement goes to both Amdel Laboratories (Adelaide), who provided access to their HPGR test unit, and Krupp Polysius (Germany) who manufactured the new studded rolls for Amdel. The use of the laboratory-scale test unit was of paramount importance to the HPGR model verification research project.

P.J. Sergeant of De Beers and M. Rylatt of BHP Billiton are also gratefully acknowledged for the supply of ore samples and corresponding industrial scale operational data. R. Shaw of Rio Tinto is also acknowledged for allowing access to experimental data from a previous research project. Without the committed involvement of these companies, this project would not have been possible.

References

AMIRA P428, 1996, Application of High Pressure Grinding rolls in Mineral Processing, Final report P428/11, Confidential, Jul/Aug 1996.

Battersby, M.J.G., Kellerwessel, H. and Oberheuser, G., 1992. Important advances in the development of high pressure rolls comminution for the minerals industry. Extractive Metallurgy of Gold and Base Metals, Kalgoorlie, Australia, pp 159-165

Farahmand, A and Ehrentraut, G,1997, Erzmetall, No. 3/March 1997, p 201-210.

Fuerstenau, D. W., Shukla, A. and Kapur, P.C., 1991. Energy consumption and product size distributions in choke-fed, high-compression roll mills. International Journal of Mineral Processing, 32, pp 59-79

Fuerstenau, D.W., Kapur, P.C., and Gutsche, O., 1993. Comminution of single particles in a rigidly-mounted roll mill Part 1: Mill torque model and energy investment. Powder Technology, 76, pp 253-262

Lim, W.I.L. and Weller, K.R.,1997 b, Modelling of throughput in the high pressure grinding rolls. In the proceedings of the XX International Mineral Processing Congress(IMPC), Aachen, Germany, September 1997, pg 173-184.

Morrell, S.; Lim, W.I.L.; Tondo, L.A.; David, D;1996, Modelling the high pressure grinding rolls, Mining technology conference, pp 169-176

Morrell, S., Shi, F., Tondo, L.A., 1997, Modelling and Scale-up of High Pressure Grinding Rolls, In the proceedings of the XX International Mineral Processing Congress(IMPC), Aachen, Germany, September 1997.

Napier-Munn, T.J., Morrell, S., Morrison, R.D. and Kojovic, T., 1996. Mineral comminution circuits - their operation and optimisation. Julius Kruttschnitt Mineral Research Centre, Monograph, Vol. 2, The University of Queensland, Brisbane, Australia, pp.149.

Schönert, K, Sander, U.;2001, Shear stresses and material slip in high pressure roller mills, Elsevier, Powder Technology 122 (2002) 136-144, March (2001).

Schönert, K., 1988. A first survey of grinding with high-compression roller mills. International Journal of Mineral Processing., 22: 401-412

Schönert, K., 1991. Advances in comminution fundamental, and impacts on technology, XVII International Mineral Processing Congress, Dresden, Sept 23-28 1991, Volume 1, pp 1-21.

Schönert, K.; Sander, U., 2000, Pressure and shear on the roller surfaces of high pressure roller mills., Proceedings of the XXI International Mineral Processing Congress, Rome, Italy, sect A4, pp 97-103

Tondo, L.A.;1997,Phenomenological modelling of a high pressure grinding roll mill, MSc Thesis, Julius Kruttschnitt Mineral Research Centre, Department of Mining and Metallurgical Engineering, University of Queensland.

Watson, S. and Brooks, M., 1994. KCGM Evaluation of High Pressure Grinding Roll Technology. Fifth Mill Operators' Conference, Roxby Downs SA, pp 69-83.